

UC Berkeley

UC Berkeley Previously Published Works

Title

Seasonal trends in photosynthesis and electron transport during the Mediterranean summer drought in leaves of deciduous oaks

Permalink

<https://escholarship.org/uc/item/4vj7t18q>

Journal

Tree Physiology, 35(5)

ISSN

0829-318X

Authors

Osuna, Jessica L
Baldocchi, Dennis D
Kobayashi, Hideki
et al.

Publication Date

2015-05-01

DOI

10.1093/treephys/tpv023

Peer reviewed



Tree Physiology 00, 1–16
doi:10.1093/treephys/tpv023

Research paper

Seasonal trends in photosynthesis and electron transport during the Mediterranean summer drought in leaves of deciduous oaks

Jessica L. Osuna^{1,2,4}, Dennis D. Baldocchi¹, Hideki Kobayashi^{1,3} and Todd E. Dawson¹

¹Ecosystem Science Division, Department of Environmental Science, Policy and Management, University of California Berkeley, Berkeley, CA, USA; ²Present address: Atmospheric, Earth, and Energy Division, Lawrence Livermore National Laboratory, PO Box 888, L-103, Livermore, CA 94551, USA; ³Present address: Department of Environmental Geochemical Cycle Research, Japan Agency for Marine-Earth Science and Technology, 3173-25 Showa machi, Kanazawa-ku, Yokohama 236-0001, Japan; ⁴Corresponding author (osuna2@lbnl.gov)

Received November 7, 2014; accepted February 25, 2015; handling Editor Jörg-Peter Schnitzler

The California Mediterranean savanna has harsh summer conditions with minimal soil moisture, high temperature, high incoming solar radiation and little or no precipitation. Deciduous blue oaks, *Quercus douglasii* Hook. and Arn., are winter-deciduous obligate phreatophytes, transpiring mostly groundwater throughout the summer drought. The objective of this work is to fully characterize the seasonal trends of photosynthesis in blue oaks as well as the mechanistic relationships between leaf structure and function. We estimate radiative load of the leaves via the FLiES model and perform in situ measurements of leaf water potential, leaf nitrogen content, an index of chlorophyll content (SPAD readings), photosynthetic and electron transport capacity, and instantaneous rates of CO₂ assimilation and electron transport. We measured multiple trees over 3 years providing data from a range of conditions. Our study included one individual that demonstrated strong drought stress as indicated by changes in SPAD readings, leaf nitrogen and all measures of leaf functioning. In the year following severe environmental stress, one individual altered foliation patterns on the crown but did not die. In all other individuals, we found that net carbon assimilation and photosynthetic capacity decreased during the summer drought. SPAD values, electron transport rate (ETR) and quantum yield of photosystem II (PSII) did not show a strong decrease during the summer drought. In most individuals, PSII activity and SPAD readings did not indicate leaf structural or functional damage throughout the season. While net carbon assimilation was tightly coupled to stomatal conductance, the coupling was not as tight with ETR possibly due to contributions from photorespiration or other protective processes. Our work demonstrates that the blue oaks avoid structural damage by maintaining the capacity to convert and dissipate incoming solar radiation during the hot summer drought and are effective at fixing carbon by maximizing rates during the mild spring conditions.

Keywords: blue oak, drought, environmental stress, fluorescence, groundwater, photosynthetic capacity, phreatophyte, PSII, *Quercus douglasii*, savanna, V_{cmax}

Introduction

The blue oak (*Quercus douglasii* Hook. and Arn.) savanna of California occurs in a region that is annually subjected to drought while also consistently receiving large amounts of incoming solar radiation. As this region is highly sensitive to climate change (Kueppers et al. 2005), predictions in changes of precipitation for the region vary, ranging from a 9% decrease to a 10%

increase in precipitation (Dai et al. 2001, Cayan et al. 2008). Kueppers et al. (2005) used a fine-resolution regional climate model to predict changes in suitable habitat for blue oaks. Because of the predicted decrease in spring and summer precipitation along with an increase in summer temperature, stronger droughts are predicted and suitable habitat for blue oaks was therefore predicted to decrease by 41%. However, the extent of drought that blue oaks can withstand is not entirely

clear and may also depend on changes in the availability of groundwater, as groundwater provides the lifeline for persistence through annual summer drought (Miller et al. 2010). Because the trees are winter deciduous, the growing season begins in the spring when soil moisture is often high. The moisture rapidly depletes and the majority of the period of foliation coincides with a period of extremely low soil moisture, negligible precipitation, high incoming solar radiation and high air temperatures (Xu and Baldocchi 2004). Seasonal adjustments in leaf structure and function enable evergreen Mediterranean species to survive the annual summer drought (Tenhunen et al. 1985, 1990, Werner et al. 2001, Wright et al. 2004, Limousin et al. 2010, Misson et al. 2010). Much less is known, however, about leaf level adjustments in winter-deciduous Mediterranean species (Damesin and Rambal 1995, Damesin et al. 1998, Xu and Baldocchi 2003). As such, it is important to understand how the blue oaks are functioning—both in terms of net carbon assimilation and conversion or dissipation of absorbed photosynthetic photon flux density (PPFD)—under the current annual drought in order to understand how future drought scenarios may affect them.

The California Mediterranean oak savanna is a particularly harsh environment. Air temperatures can reach or even exceed 40 °C. Volumetric soil moisture is at or below 10% throughout most of the period of foliation (Baldocchi et al. 2006, Chen et al. 2008b) with leaf water potential reaching as low as -7 MPa (Xu and Baldocchi 2003). Air temperature, leaf-to-air vapor pressure deficit and PPFD remain high throughout the summer (Kobayashi et al. 2012). Despite these conditions leaves persist on the trees well into the fall (Ryu et al. 2012) and the site is consistently a net carbon sink (Ma et al. 2007). With recorded photosynthetic capacity up to $127 \mu\text{mol m}^{-2} \text{s}^{-1}$, blue oaks have among the highest capacity recorded of broad-leaved trees, especially those from Mediterranean regions (Wullschlegel 1993, Xu and Baldocchi 2003, Misson et al. 2010). This conundrum of high photosynthetic capacity during extreme drought results in ecosystem models consistently underestimating uptake of CO_2 at deciduous, drought-stressed ecosystems (Vargas et al. 2013). Two factors that may contribute to the underperformance of ecosystem flux models at Mediterranean sites with a deciduous canopy are (i) the strong peak and seasonality of photosynthetic capacity and (ii) the complex relationship between soil moisture, groundwater and vegetation.

In a previous study of the ecohydrology of deciduous oak grassland, Miller et al. (2010) found that surface soil moisture was the greatest source of transpired water during the spring. This source is rapidly and consistently depleted during the summer (Ma et al. 2011). Groundwater accounted for 97% of water transpired by the deciduous oaks during the summer drought, however actual transpiration rates were very low (Miller et al. 2010). Blue oaks are obligate phreatophytes, using groundwater for at least 6 months of the year (Miller et al. 2010). The work of

Miller et al. (2010) indicated groundwater uptake in 2008 at $18\text{--}25 \text{ mm month}^{-1}$ from April through July, and then at 12 mm month^{-1} . The extent of blue oak coarse and fine root systems are related to crown size (Raz-Yaseef et al. 2013, Koteen et al. 2014), and thus crown size may also indicate the degree to which a tree is able to access groundwater. Reduced transpiration rates during the summer coincide with down-regulated carboxylation capacity (Xu and Baldocchi 2003). A reduction of carboxylation capacity is often a response of extended severe drought and can be partially due to a reduction of Rubisco content (Lawlor and Tezara 2009 and citations within).

While the summer drought results in reduced net carbon assimilation in the California oak savanna, the lack of cloud cover and precipitation result in abundant PPFD and high summer temperatures. The Farquhar, von Caemmerer and Berry model of photosynthesis (Farquhar et al. 1980), further described by Bernacchi et al. (2001), showed that as temperature increases, Rubisco carboxylation decreases relative to oxygenation, effectively decreasing net assimilation. Photosystem II (PSII) often remains intact during drought and can efficiently convert absorbed PPFD to avoid photo-oxidative damage, even during extreme droughts, resulting in decreased photosynthetic capacity and stomatal conductance (Damour et al. 2009). However, high temperatures can damage PSII and when accompanied by severe drought stress, plants are more susceptible to this damage (Hamerlynck et al. 2000). Based on the variable relationship between photosynthetic capacity and maximum electron transport rate (ETR), Xu and Baldocchi (2003) concluded that structural and biochemical damage from excess PPFD contributed to a decrease in photosynthetic capacity and therefore photosynthesis in blue oaks during the summer drought.

The objective of this work is to investigate the mechanistic associations between photosynthesis and the capacity to convert or dissipate PPFD in order to better understand controls over leaf functioning throughout the annual hot summer drought of the California Mediterranean savanna. Our work leverages information from previous work on seasonal trends in photosynthetic parameters (Xu and Baldocchi 2003), blue oak access to groundwater (Miller et al. 2010) and coarse and fine root distribution of the blue oaks (Raz-Yaseef et al. 2013, Koteen et al. 2014). Here, we performed a broad suite of measurements including leaf water potential, solar irradiance, leaf nitrogen content, leaf absorptance, apparent quantum yield, dark respiration, light-saturated photosynthesis, photosynthetic capacity, maximum electron transport and actual ETR. We performed these measurements on multiple trees at the site throughout multiple years and therefore captured a range of water availability. Through this suite of measurements, we are able to assess relative and actual reductions in net carbon assimilation and electron transport throughout the summer drought. Additionally, we could assess whether these reductions are a result of damage to the biochemical or structural integrity of the leaf, or a strategic adjustment for surviving the annual drought.

We predict that while photosynthesis decreases during the summer drought, the leaf structures involved in converting PPFD to energy remain intact and fully functional, thus avoiding leaf damage. Considering that blue oaks have survived the annual California Mediterranean drought over long periods of time, we interpret the seasonal trends as strategic adjustments rather than an effect of damage. As such, this work can contribute to modeling the blue oak functional response to changes in environmental drivers. While leaf damage may be only very slowly reversed or irreversible, strategic adjustments may present a level of plasticity allowing for blue oaks to adjust functional responses to changes in environmental drivers.

Materials and methods

Site description

The study site is a blue oak stand at the Tonzi AmeriFlux site in the California Mediterranean savanna located near Lone, CA, USA (Baldocchi et al. 2004, Xu and Baldocchi 2004). The Tonzi Ranch rests in the lower foothills of the Sierra Nevada Mountain range (38.438°N, 120.968°W) at an altitude of 177 m. The Mediterranean climate at the site features a wet, mild winter and a dry, hot summer. From 2001 to 2009, the average annual precipitation—predominantly winter rainfall—was 534.30 mm, and the average annual temperature was 16.66 °C (Table 1). The temperature during the years of the studies did not vary greatly from this 8-year mean. In 2007, a passing cold front resulted in unseasonably cold temperatures, reaching as low as −1.8 °C on day of year (DOY) 108–2007—a relevant consideration that will be discussed further in the Results section below.

The tree canopy covers 40% of the landscape and is primarily blue oak—a winter-deciduous oak endemic to California—interspersed with occasional *Pinus sabiniana* (grey pine). Exotic annual C3 grasses and herbs make up the understory and are active during the winter and spring. The leaf area index of the tree canopy in the study area is 0.77 m² m⁻² (Ryu et al. 2010). The mean tree diameter at breast height (DBH) was 26.0 cm with a standard deviation of 11 cm (Chen et al. 2008a); mean tree height was 9.41 ± 4.33 m, and leaf size was 5.1 ± 1.8 cm² ($n = 164$) (Table 2).

Measurements were made on a total of seven trees throughout the study. Individuals were chosen intentionally, with priority

given to trees with foliage accessible from the ground, a period of direct incoming solar radiation during the morning, sufficient foliage to destructively sample leaves, and a crown shape and height typical of the stand. Some individuals rotated into or out of the sampling plan across years due to changes in foliage (discussed further in Leaf structure and Leaf function sections). We refer to trees by their numbers at the site in order to enable comparisons with other work. T92 was previously measured in the work of Xu and Baldocchi (2003).

Throughout the study, spring rainfall decreased dramatically from 329.2 mm in 2006 to 8.1 mm in 2008, a decrease of nearly 98% (Table 1). This difference in spring precipitation resulted in higher sustained soil moisture in 2006 both at the surface and at 50 cm (Figure 1). The soil dried to −0.16 cm³ cm⁻³ at 50 cm soon after DOY 140 in all 3 years and to 0.07 cm³ cm⁻³ at the surface in all years although the dry-down at the surface took nearly 2 months longer in 2006 due to the higher precipitation during the spring.

The blue oaks at Tonzi are obligate phreatophytes, using groundwater for at least 6 months of the year (Miller et al. 2010), indicating their deep and expansive (Raz-Yaseef et al. 2013, Koteen et al. 2014) rooting system. The groundwater depth at the site varies spatially and temporally but ranges from 7 to 12 m below the surface (Miller et al. 2010).

Leaf water potential Leaf water potential was measured three times on each of two (2007) or three (2008) trees at pre-dawn (Ψ_{PD}) and at mid-day (Ψ_{MD}) with a portable plant water status console (3005-Series, Soil Moisture Equipment Corp., Santa Barbara, CA, USA). Measurements were taken approximately every 10 days throughout the spring and summer for a total of 12 (2007) and 8 (2008) measurement days in each year. In

Table 2. Tree structure. DBH, average leaf area and the crown shape of the trees on which gas-exchange measurements were made, as well as stand averages (Chen et al. 2008).

| Tree | DBH (cm) | Leaf area (cm) | Crown shape |
|------------|----------|----------------|-------------|
| 35 | 65 | 5.5 ± 2.4 | Spherical |
| 92 | 226 | 4.7 ± 1.3 | Spherical |
| 228 | 95 | 4.5 ± 0.79 | Oval |
| 295 | 86 | 4.9 ± 1.2 | Oval |
| Stand avg. | 26 ± 11 | 5.1 ± 1.8 | |

Table 1. Site climate. Average annual air temperature, total precipitation in the water year (DOY 296–295), average spring temperature (defined as DOY 80–150), average spring precipitation, average summer temperature (DOY 151–260), average summer precipitation, average soil moisture in the spring at the surface (DOY 80–90) and average soil moisture in the summer at the surface (DOY 200–220).

| | Avg. temp. (°C) | Precip (mm) | Spring Temp (°C) | Spring Precip. (mm) | Summer Temp (°C) | Summer Precip. (mm) | Spring θ surface (cm ³ cm ⁻³) | Summer θ surface (cm ³ cm ⁻³) |
|---------|-----------------|-------------|------------------|---------------------|------------------|---------------------|---|---|
| 2006 | 16.3 | 881.4 | 15.3 | 329.2 | 24.1 | 0 | 0.46 | 0.070 |
| 2007 | 16.1 | 405.1 | 16.2 | 100.1 | 23.2 | 0.3 | 0.30 | 0.061 |
| 2008 | 16.4 | 379.7 | 15.8 | 8.1 | 23.3 | 0.5 | 0.28 | 0.061 |
| 2001–09 | 16.7 | 534.3 | 15.6 | 114.5 | 23.7 | 6.4 | 0.39 | 0.059 |

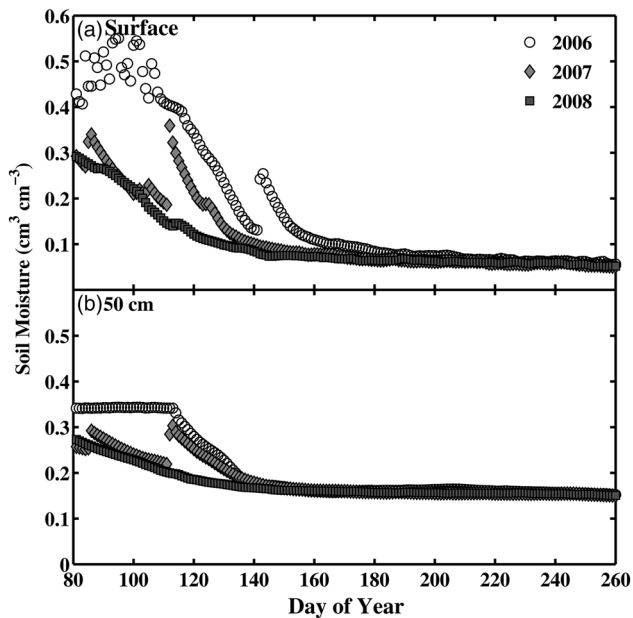


Figure 1. Soil moisture from the Tonzi AmeriFlux site at the surface (a) and 50 cm (b). Measurements are shown from 2006 (circles), 2007 (diamonds) and 2008 (squares).

2007, two trees (T102 and T255) were chosen based upon their representativeness of the site and the accessibility of foliage on the south side of the tree (see Leaf function section). T92 was added to the measurements in 2008.

Solar radiation exposure On each tree used for gas-exchange measurements (T35, T92, T228 and T295; discussed more in Leaf structure and Leaf function sections), we modeled the duration of full sun exposure and total photosynthetically active radiation (PAR) received throughout the day using FLIES, a three-dimensional radiative transfer model (Kobayashi and Iwabuchi 2008, Kobayashi et al. 2012). We chose this model because it has previously been shown to compute the radiation environment for this site particularly accurately and because the radiation environment of individual trees is explicitly simulated (Kobayashi et al. 2012). Using both satellite and airborne-Light Detection and Ranging (LiDAR) data, we isolated the lower south side of the crown that was used for gas-exchange measurements. We modeled 1 day each in spring and summer (DOYs 109-2008 and 206-2008).

Leaf structure

Measurements of leaf structure were made on four trees in 2006 (12 measurements from DOY 117–251), 2007 (14 measurements from DOY 95–234) and 2008 (16 measurements from DOY 95–248). T92 and T35 were included every year. T101 and T102 were sampled in 2006, replaced by T228 and T295 in following years to coordinate with gas-exchange measurements.

Leaf nitrogen and chlorophyll content Total leaf area of four leaves from each tree was measured using a LI-3100 (Li-Cor, Lincoln, NE, USA). Leaves were dried and weighed to calculate leaf mass per area (LMA) before measuring leaf nitrogen content on a mass basis via elemental analyzer (ANCA/SL elemental analyzer, Sercon, Cheshire, UK). All analyses were conducted at the Center for Stable Isotope Biogeochemistry at the University of California, Berkeley. In 2008, we measured an index of chlorophyll content of 12 intact leaves per tree, including the four collected for LMA and leaf nitrogen, using a SPAD-502 Chlorophyll Meter (Spectrum Technologies, Inc., Plainfield, IL, USA).

Leaf absorbance An LI-1800-12S Integrating Sphere (Li-Cor) and a USB2000 Fiber Optic Spectrometer (Ocean Optics Inc., Dunedin, FL, USA) were used to measure leaf transmittance (T_L) and reflectance (R_L) of four leaves in order to calculate leaf absorbance:

$$1 = T_L + R_L + \alpha_L, \quad (1)$$

where α_L is the full leaf absorbance spectra. For calculation of electron transport, we then calculated leaf absorbance as a weighted average of the absorbance over the spectra of light received by the leaves (further details given below in Leaf function section).

Leaf function

Leaf gas exchange and fluorescence were measured using an LI-6400-40 Portable Photosynthesis System with integrated fluorescence measurements (Li-Cor). To extend Xu and Baldocchi's investigation (2003), we gathered leaf-function data on the same tree (T92) in 2006. In 2007, measurements were performed on T35, T228 and T295. T228 and T295 were chosen because they both have cylindrical shaped crowns that are typical of the stand and receive full sunlight in the morning; T35 was chosen because it has a broad, spherical crown similar to T92 (but atypical for the stand) and receives full sunlight in the morning. The intention of the sampling strategy in 2007 was to determine whether the trends observed in T92 were consistent with trends in other individuals at the site. Crown size was the dominant factor affecting our choice of trees to sample because crown size is associated with root biomass (Koteen et al. 2014). In 2008, measurements were performed on T92, T228 and T295—T35 was not measured due to a lack of accessible foliage in 2008 (see Discussion section). All measurements were performed on an accessible clump of leaves on the south side of the tree.

Light response curves Net CO_2 assimilation rate, A , was measured at 11 levels of PPFD from 0 to $2500 \mu\text{mol m}^{-2} \text{s}^{-1}$, and additionally at $3000 \mu\text{mol m}^{-2} \text{s}^{-1}$ on days when rates did not plateau by $2500 \mu\text{mol m}^{-2} \text{s}^{-1}$. Leaf temperature was maintained

at the initial value throughout the measurements. Using a non-rectangular hyperbola based on the works of Marshall and Biscoe (1980) and Thornley and Johnson (1990), daytime respiration in the dark (R_{dTL}) was calculated from light response curves via a macro developed by Kevin Tu (available at <http://www.landflux.org/tools.php>). We adjusted R_{dTL} to 25 °C (R_{d25}) with the Arrhenius equation, assuming a constant activation energy (E_a):

$$R_{dTL} = R_{d25} \exp\left(\frac{E_a}{R} (298.15^{-1} - T_{LK}^{-1})\right), \quad (2)$$

where R is the universal gas constant, E_a is assigned a value of 66.4 kJ mol⁻¹ (Von Caemmerer 2000) and T_{LK} is the leaf temperature in degrees Kelvin.

CO₂ response curves $A-C_i$ curves (response of A to changes in intercellular CO₂ concentration) were measured on intact leaves following light response curves. Photosynthetic photon flux density in the leaf chamber was set to the minimal saturating level and CO₂ in the chamber was set to 380 ppm. Leaf temperature was set to maintain the initial ambient leaf temperature. Measurements were made at 380, 400, 750, 1000, 1300, 350, 200, 50, 150, 250 and 400 ppm. Measurements were made in this order to minimize hysteresis at the upper portion of the curve, fully characterize the initial slope and keep measurement duration to <1 h per curve.

To analyze the $A-C_i$ curves, we used the tool of Sharkey et al. (2007), an estimator utility available at <http://www.blackwellpublishing.com/plantsci/pcecalculation>. This method was chosen because: (i) the program allows the user to choose the range for each of the three photosynthetic limitations: Rubisco-limited (initially $C_i < 200$ ppm), RuBP-regeneration-limited (initially $C_i > 300$ ppm) and triose phosphate use-limited (highest CO₂ partial pressure from the plateau portion of the response curve); and (ii) the program allows for the input of any parameters that are independently known, improving the estimation of the other parameters. For most curves, the published guidelines were appropriate for assigning limiting factors, although some cases required reassignment to avoid inclusion of co-limited regions of the curve. Estimates of the maximum rate of carboxylation, V_{cmax} , and electron transport, J_{max} , were adjusted to 25 °C in the Sharkey tool based on equations from Harley et al. (1992).

Following the methods of Farquhar et al. (1980), V_{cmax} was calculated as the slope of the initial linear portion of the response curve (Rubisco-limited values):

$$A = V_{cmax} \left[\frac{c_c - \Gamma^*}{c_c + K_C(1 + (O/K_O))} \right] - R_d, \quad (3)$$

where c_c is the partial pressure of CO₂ at the site of carboxylation (calculated as described below), K_C and K_O are the Michaelis–Menten constant of Rubisco for CO₂ and O₂, respectively, Γ^*

is the compensation point between release of CO₂ via photorespiration (non-mitochondrial) and uptake of CO₂ via photosynthetic fixation, and R_d is mitochondrial respiration during the day.

J_{max} was calculated from the linear portion of the curve at the higher values of C_i (when available):

$$A = J_{max} \left[\frac{c_c - \Gamma^*}{4c_c - 8\Gamma^*} \right] - R_d. \quad (4)$$

A non-linear curve-fitting program based on data in both the Rubisco-limited and RuBP-limited portions of the curve is used to estimate internal conductance (g_i) and R_d . The c_c value is then calculated as $(c_i - A/g_i)$. Due to low stomatal conductance occasionally resulting in c_i remaining within the range of the linear initial slope, information was not always available from the RuBP-limited portion of the curve, preventing calculation of J_{max} and g_i . R_d was not affected, however, because we used our independent estimate from light response curves measured on the same day and individual. While incomplete curves are not ideal, they are the reality of measurements taken from a site with such low water availability. While not considering internal conductance can affect the estimation of V_{cmax} and J_{max} , we were primarily interested in relative changes across the season as well as the ratio of the two parameters, which is not as affected by estimations of c_c (Miao et al. 2009).

Instantaneous photosynthesis and electron transport Steady-state photosynthesis, stomatal conductance (g_s) and ETR were measured on ~10 leaves neighboring the leaf where the response curves were measured. Photosynthetic photon flux density in the chamber was set to saturating and CO₂ was set to 380 ppm. The percentage of PPFD emitted by the blue LEDs was set to the maximum possible—normally between 10 and 20%—to stimulate higher stomatal conductance (Zeiger et al. 1985). We measured photosynthesis and leaf fluorescence immediately before initiating a saturating flash during which fluorescence was measured again. The flow of electrons through PSII per unit quantum flux, ϕ_{PSII} , was then calculated from fluorescence measurements (Genty et al. 1989):

$$\phi_{PSII} = \frac{F'_m - F_s}{F'_m}, \quad (5)$$

where F'_m is the maximum fluorescence of a light-adapted leaf and F_s is the steady-state fluorescence of a light-adapted leaf. Using Eq. (5), the gas-exchange data and leaf absorbance measurements, we calculated the total ETR (J_t) as

$$J_t = f \times \phi_{PSII} \times I_T \times \alpha_L \quad (6)$$

where f is the fraction of absorbed quanta used by PSII (presumed to be 0.5), and I_T is the incident radiation on the leaf

surface. To achieve the best possible estimation of leaf absorptance, we calculated a weighted average based on the emission spectra of the red and blue LED light sources in the LI-6400-40 (data provided by Li-Cor).

Results

Environmental drivers

Plant water status As is expected in a Mediterranean climate with no summer rain, in both years of measurements (2007–08), mid-day and pre-dawn water potential became more negative throughout the season (Figure 2). Both T102 and T255 showed an early and rapid decline in pre-dawn water potential, dropping below -2 MPa on DOY 184–2008 in both T102 and

T255, whereas the pre-dawn water potential of T92 did not drop below -2 MPa until DOY 220–2008. The within-site variability of water potential indicates a range of drought exposure. In 2007, as pre-dawn water potential became more negative, the drawdown in water potential from pre-dawn to mid-day, $\Delta\Psi$, approached 0, whereas at pre-dawn water potentials around -1 MPa $\Delta\Psi$ was -2 MPa (Figure 3). Despite a range both in pre-dawn water potential and $\Delta\Psi$ similar to 2007, there was no correlation between $\Delta\Psi$ and pre-dawn water potential in any of the trees measured.

Radiation environment According to our model estimates, T35, T92 and T295 experienced full, unobstructed sunlight for large parts of the day (Table 3) including during the morning when

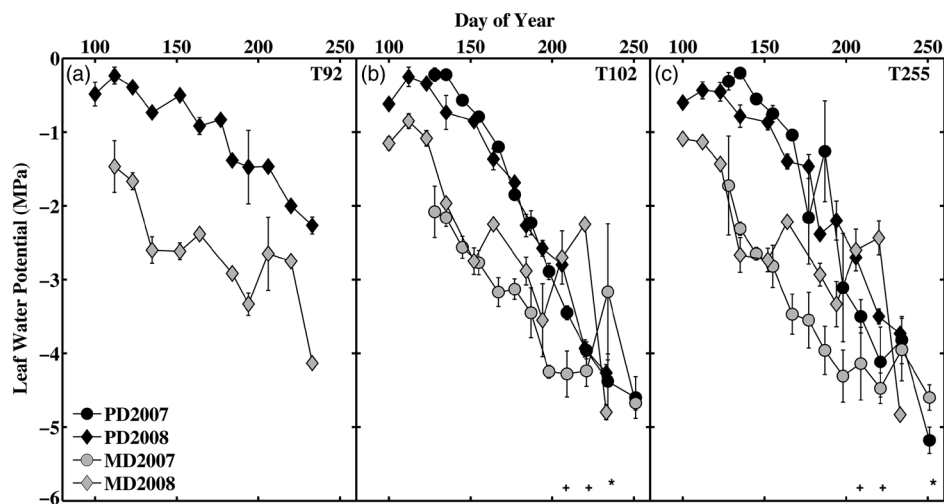


Figure 2. Seasonal progression of leaf water potential in the pre-dawn (black) and mid-day (gray) for trees 92 (a), 102 (b) and 255 (c) during 2007 (circles) and 2008 (diamonds). Each data point is the average of three measurements, with error bars indicating standard deviation. An '*' or a '+' indicates days on which the measured mid-day leaf water potential was higher than the pre-dawn leaf water potential in 2007 or 2008, respectively. These data were not excluded because the data were consistently replicated during multiple measurements on those days.

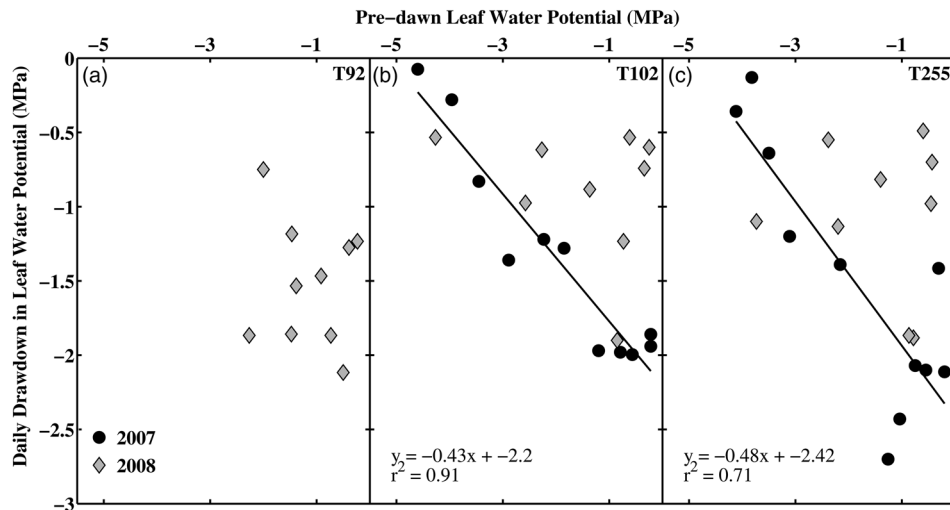


Figure 3. Daily drawdown of leaf water potential from pre-dawn to mid-day (y-axis) plotted as a function of pre-dawn leaf water potential for trees 92 (a), 102 (b) and 255 (c) in 2007 (circles) and 2008 (diamonds). The equation and fit for 2007 is shown.

Table 3. Incoming solar radiation and leaf structure in the region of gas exchange and leaf fluorescence measurements on each tree. Duration of full sun and amount of absorbed PAR (APAR), leaf mass per area (LMA), leaf nitrogen content as a percentage of mass (N_m), SPAD values and leaf absorptance in red and blue. For all values except SPAD values, the first letters indicate significance across years (vertical throughout table) and the second letters indicate significance across individuals (horizontal throughout chart) within a year; for SPAD values, only significance across individuals is shown.

| | T35 | T92 | T228 | T295 |
|---|-----------------------------|-----------------------------|----------------------------|-----------------------------|
| Hours full sunlight | | | | |
| DOY 109 | 10.5 | 9.5 | 4.8 | 11.3 |
| DOY 206 | 9.3 | 7.7 | 3.8 | 11.7 |
| Total APAR per day (mol m ⁻² day ⁻¹) | | | | |
| DOY 109 | 25.2 | 23.6 | 11.5 | 28.1 |
| DOY 206 | 23.8 | 22.6 | 11.6 | 27.5 |
| LMA ± SD (g m ⁻²) | | | | |
| 2006 | 125.8 ± 11.4 _{a,a} | 140.3 ± 7.7 _{a,b} | – | – |
| 2007 | 125.8 ± 8.8 _{a,a} | 147.0 ± 15.9 _{a,b} | 127.2 ± 4.9 _{a,a} | 149.6 ± 16.1 _{a,b} |
| 2008 | 114.0 ± 12.1 _{a,a} | 133.8 ± 15.6 _{a,b} | 122.2 ± 7.3 _{a,b} | 131.6 ± 16.2 _{b,b} |
| N_m ± SD (%) | | | | |
| 2006 | 2.00 ± 0.22 _{a,a} | 2.26 ± 0.3 _{a,a} | – | – |
| 2007 | 1.66 ± 0.16 _{b,a} | 1.99 ± 0.13 _{b,b} | 1.97 ± 0.31 _{a,b} | 2.04 ± 0.28 _{a,b} |
| 2008 | 2.26 ± 0.10 _{a,a} | 2.54 ± 0.19 _{a,b} | 2.30 ± 0.13 _{b,a} | 2.35 ± 0.15 _{b,a} |
| SPAD ± SD | | | | |
| 2008 | 40.1 ± 3.9 _a | 52.3 ± 4.7 _b | 44.5 ± 4.7 _c | 53.7 ± 4.4 _b |
| Leaf absorptance ± SD | | | | |
| Red (572–706 nm) | – | 0.90 ± 0.013 _a | 0.88 ± 0.025 _b | 0.89 ± 0.014 _{a,d} |
| Blue (432–512 nm) | – | 0.92 ± 0.009 _c | 0.91 ± 0.006 _c | 0.90 ± 0.017 _d |

measurements were made. As discussed above in the Leaf function section, T228 was chosen for study partially due to the period of full sunlight in the morning. However, the model reveals that T228 received 50% or less sunlight throughout the day compared with other individuals. This decreased incoming solar radiation will factor in to leaf structure, discussed further below.

Leaf structure

Leaf nitrogen content Leaf mass per area increased during leaf development but did not have a distinct seasonal trend throughout the remainder of the year (for this reason, the trend is not shown). Aside from in T295, inter-annual variability of LMA was insignificant (Table 3). Leaf nitrogen content by mass (N_m) was highest at leaf emergence and decreased sharply during leaf development (Figure 4). In 2007—the year of marked decline in precipitation—leaf nitrogen content decreased throughout the summer in T228 and T295. In other years and individuals, N_m remained constant throughout the summer. During 2008, leaf nitrogen was higher than other years, ranging from 2.26% (T35-2008) to 2.55% (T92-2008).

SPAD readings increased until nearly DOY 160 (Figure 5). After DOY 160, the trend was inconsistent across trees. SPAD readings in T35 and T228 slowly decreased after DOY 160 and had the lowest values, reaching ~35 by the end of measurements. T92 and T295 had SPAD readings from 50 to 55 throughout most of the summer, with no clear temporal trend. The tendency for standard deviation to increase throughout the summer may be attributable to leaves progressing toward senescence at different rates.

Leaf absorptance No discernable seasonal trend was present in leaf absorptance. Averaged values of absorptance in each blue and red were used to calculate ETR in 2006 and 2007 when leaf absorptance was not measured (Table 3). In 2008, we used the measured value of leaf absorptance from the same day and individual for calculating electron transport.

Leaf function

Light response curves The light response curves demonstrated that A peaked at high levels of PPFD, sometimes not peaking by 3000 $\mu\text{mol photons m}^{-2} \text{s}^{-1}$, the maximum PPFD achievable with the LI-6400-40 and well beyond the solar constant. Only T35 demonstrated A consistently saturating below 3000 $\mu\text{mol photons m}^{-2} \text{s}^{-1}$. Unsaturated curves primarily occurred during the spring, meaning that reported 'maximum' values may not actually indicate light-saturated A . Figure 6a–c shows that light-saturated net assimilation tended to be higher during the spring, with values reaching 22 $\mu\text{mol m}^{-2} \text{s}^{-1}$ (T92-2006). In the 3 years of measurements, only T35 in 2007 exhibited photoinhibition via a decrease of A at high PPFD.

Despite high incident solar radiation, the efficiency with which PPFD was used for net carbon assimilation, apparent quantum yield $\phi_{A'}$, decreased throughout summer in 2007 and 2008, excluding data from DOY 108-2007 when the cold front passed as described in Environmental drivers section above (Figure 6d–f). The lowest $\phi_{A'}$ measured was on DOY 177-2007 in T35, possibly due to measuring a leaf that was experiencing biochemical and physical breakdown associated with senescence despite

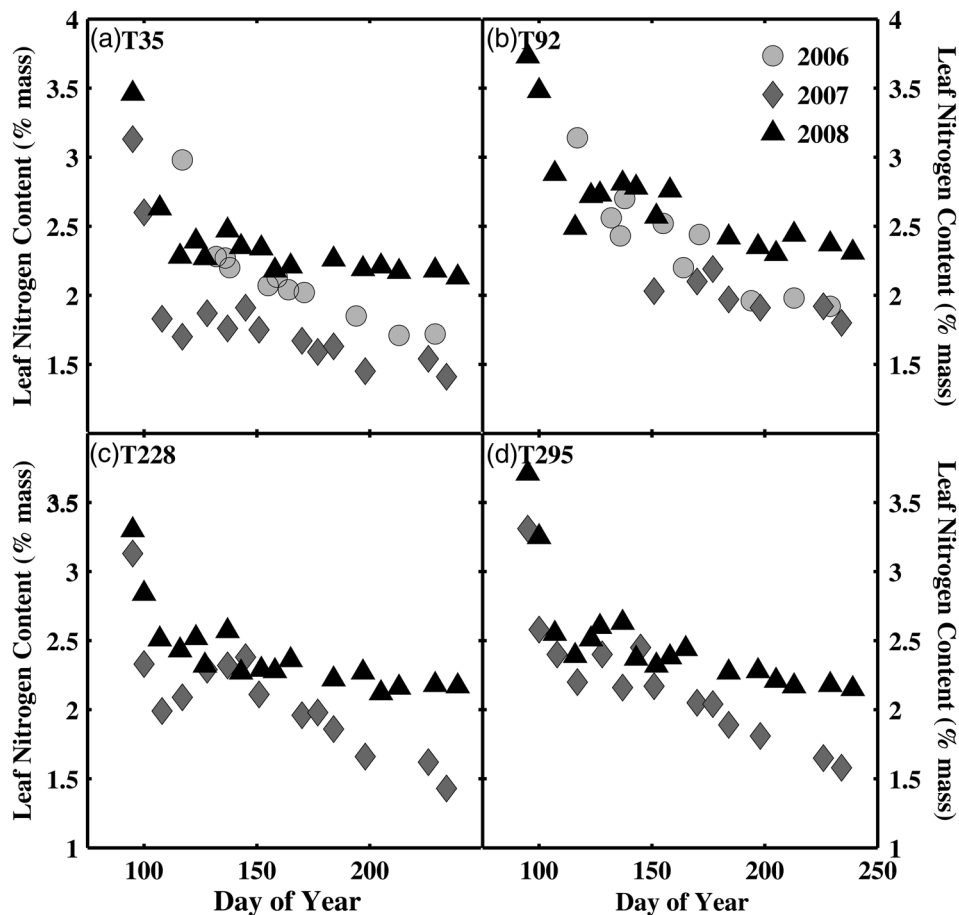


Figure 4. Leaf nitrogen content on a mass basis for trees 35 (a), 92 (b), 228 (c) and 295 (d) during 2006 (circles), 2007 (diamonds) and 2008 (triangles). Each data point was measured based on a combined sample from ~3 to 4 leaves collected from the region where leaf gas-exchange and fluorescence measurements were made.

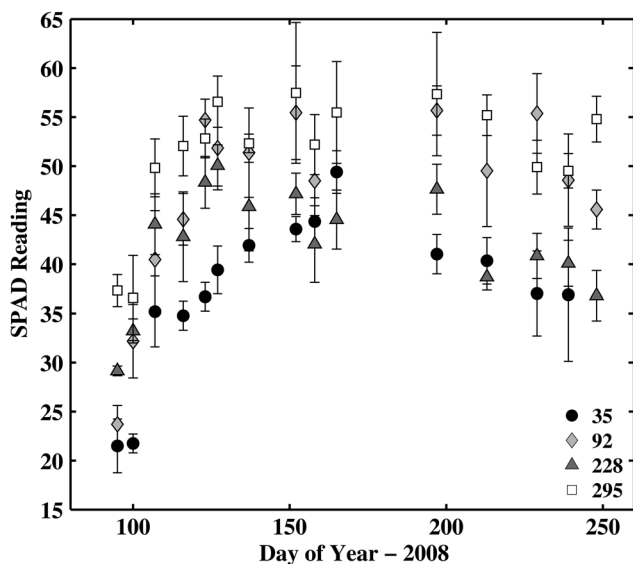


Figure 5. SPAD readings, an index of leaf chlorophyll content, in 2008 for trees 35, 92, 228 and 295. Each data point is the average of measurements from 12 leaves located in the region of leaf gas-exchange and fluorescence measurements. Error bars indicate standard deviation.

visibly appearing healthy. In 2006, ϕ_A of T92 did not decrease in the summer.

Dark respiration adjusted to 25 °C decreased exponentially throughout the season (Figure 6g–i) with little variation across years or individuals. R_{d25} decreased more rapidly in T35 than in other individuals. On DOY 108-2007 when the cold front passed, R_{d25} was suppressed in T228.

CO₂ response curves V_{cmax} followed the seasonal trend previously reported for the site (Xu and Baldocchi 2003), peaking in the spring each year. The trend in J_{max} also peaked in the spring (Figure 7). The maximum temperature-adjusted V_{cmax} and J_{max} observed were 130 and 195 $\mu\text{mol m}^{-2} \text{s}^{-1}$, respectively, on DOY 127-2008 in T92. The Sharkey tool was not able to calculate internal conductance for most of the A–C_i curves produced in this study due to the low stomatal conductance often resulting in unsaturated curves, as discussed in the Leaf function section. The high V_{cmax} and J_{max} demonstrate that to prosper, these oaks attain high capacity to acquire enough carbon during the ideal conditions of spring in order to sustain them during the long summer drought when rates of photosynthesis are lower.

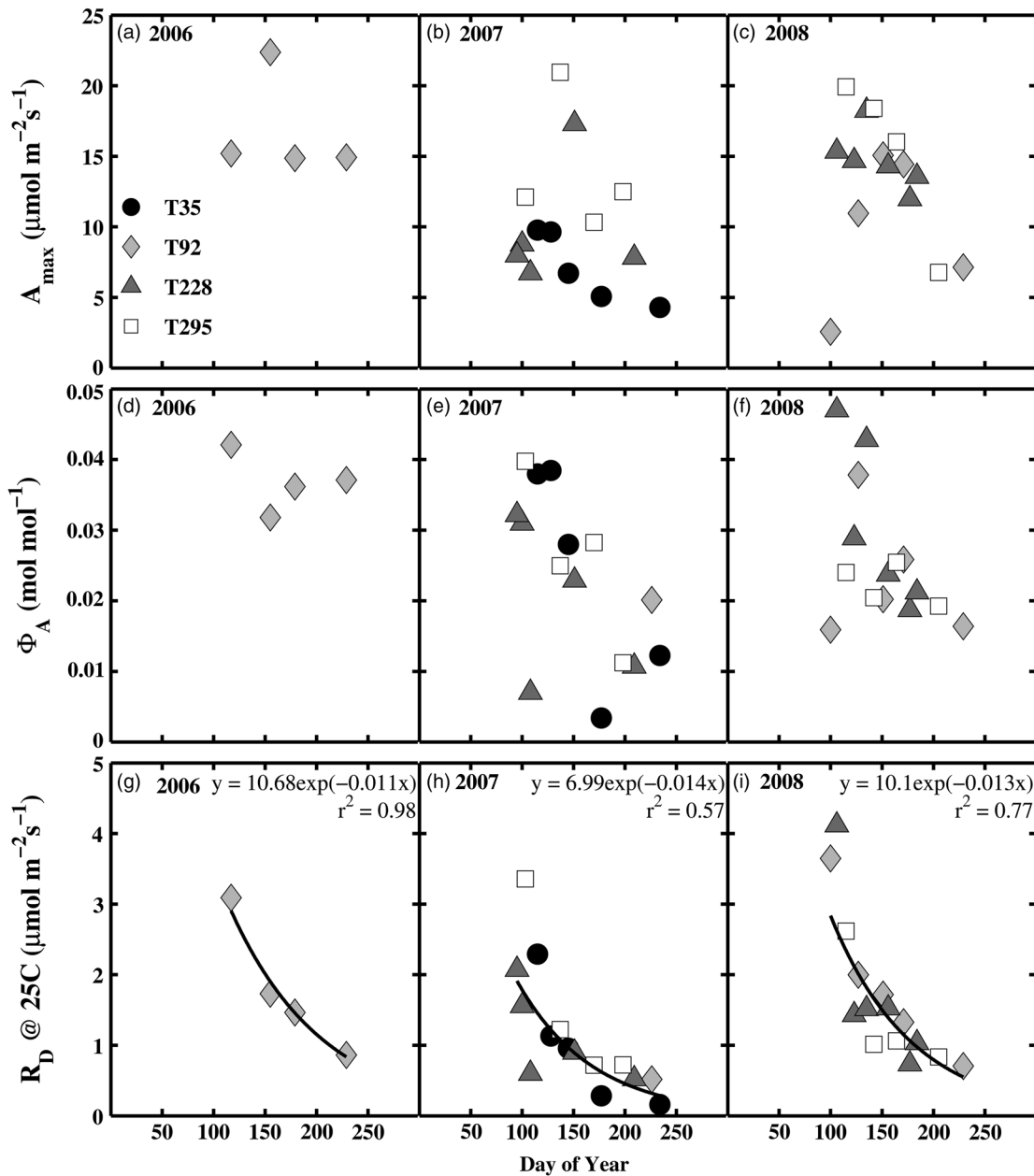


Figure 6. Light-saturated net assimilation rate (a–c), apparent quantum yield of net CO₂ assimilation (d–f) and dark respiration adjusted to 25 °C (g–i) of trees 35 (circles), 92 (diamonds), 228 (triangles) and 295 (squares) in 2006 (left), 2007 (middle) and 2008 (right).

Instantaneous gas-exchange and fluorescence The fraction of absorbed solar radiation used for photochemistry, ϕ_{PSII} , was maximum during the spring and decreased throughout the summer (Figure 8a–c). T228, the individual with the shortest daily period of full light exposure, had significantly higher ϕ_{PSII} during the spring of 2007. In all trees, the actual rate of electron transport also tended to be the highest during the spring (Figure 8d–f). The instantaneous rates of net carbon assimilation decreased from the peak period in spring through the summer (Figure 8g–i), accompanied by a decrease in stomatal conductance (Figure 8j–l). T92 had the highest stomatal conductance throughout the study, especially in 2006 when values were lower in the summer than

spring but did not continually decrease. This trend was associated with a similar trend in photosynthesis in 2006, wherein the summer value of $\sim 10 \mu\text{mol m}^{-2} \text{s}^{-1}$ was maintained throughout the season.

Discussion

Within-site variability of groundwater access is evident in the water potential measurements done in this study. Previous efforts were made to quantitatively assess individual tree access to groundwater via isotopic analysis, however the results were inconclusive (Miller et al. 2010). As such, the best indication of

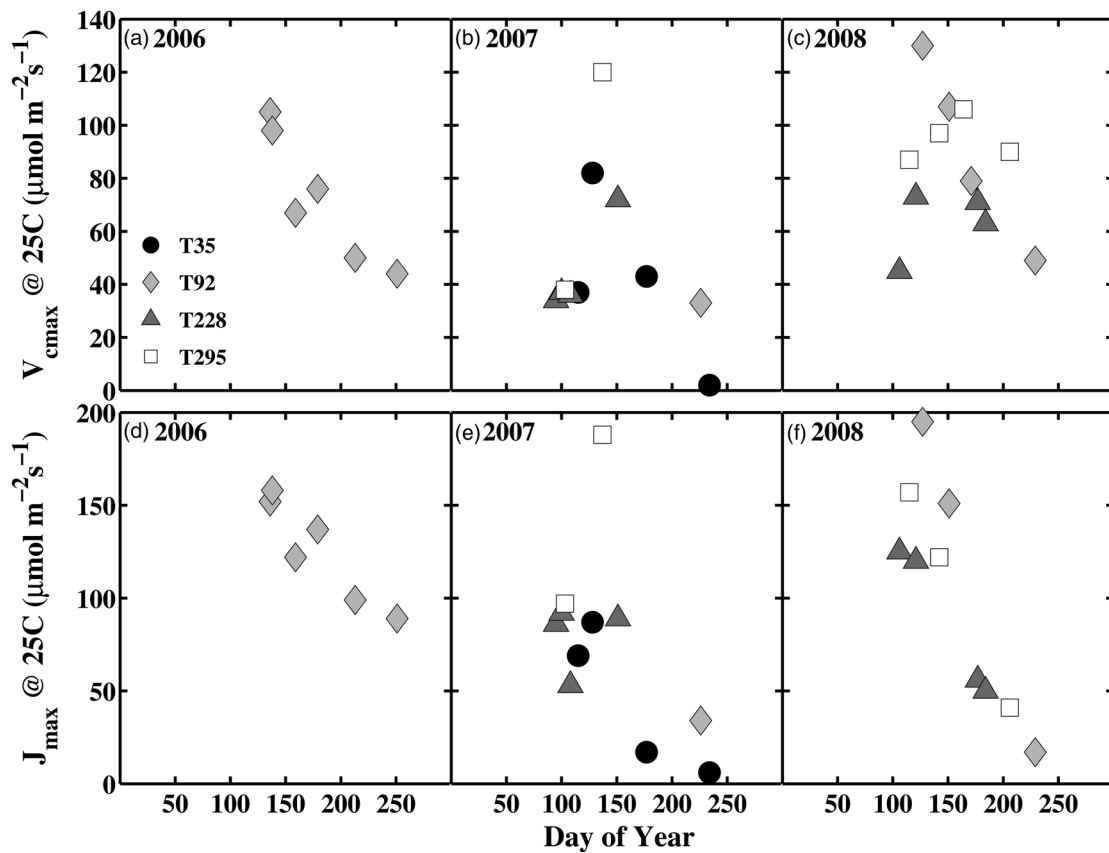


Figure 7. Photosynthetic capacity from $A-C_i$ as calculated from the Sharkey et al. (2007) method. Maximum carboxylation velocity (V_{cmax} , a–c) and the maximum rate of electron transport (J_{max} , d–f) are shown for 2006 (left), 2007 (middle) and 2008 (right) for T35 (circles), T92 (diamonds), T228 (triangles) and T295 (squares). All values are adjusted to 25 °C.

individual tree access to groundwater comes from leaf water potential measurements. In 2008, despite Ψ_{PD} at or above -3 MPa in T92, T102 and T255 throughout nearly the entire summer, $\Delta\Psi$ was much higher in T92 than in other trees. Higher $\Delta\Psi$ indicates that T92 was transpiring more water during the day and able to ease tension within the water column at night. Our data show that the variability in drawdown of leaf water potential throughout the summer is most likely related to variability in access to groundwater. Spatial heterogeneity in groundwater access is expected due to the variability in soil and rock layers at the site. Ground-penetrating radar data from the site shows the variability in soil depth (Raz-Yaseef et al. 2013). Additionally, the roots likely access groundwater by penetrating through fractures in the rock layers under the soil (Miller et al. 2010), adding to the spatial heterogeneity of the site.

Our data do not indicate PSII damage during the hot summer drought. While ETR decreased slightly beyond the spring peak period, PSII appeared capable of supplying energy throughout the growing season. Electron transport rate increased linearly with A (Figure 9); however, the relationship only accounted for 53% of the variability in ETR—at low A , the variability of ETR tended to be high. The higher variability of ETR at low A

demonstrates the increased contribution of sinks other than net carbon assimilation during periods of reduced A (Figure 9). The two main energy carriers produced by the electron transport chain are adenosine triphosphate (ATP) and nicotinamide adenine dinucleotide phosphate (NADPH); these compounds are also used by photorespiration, which we hypothesize is a key contributor to avoiding excessive excitation of PSII when carbon assimilation is limited (Martínez-Ferri et al. 2000) and leaf temperatures are high (Von Caemmerer 2000). Our work does not provide enough information to specifically attribute processes for alternative electron sinks. More research into alternative electron sinks in blue oaks appears to be warranted.

Net carbon assimilation was tightly coupled with stomatal conductance (Figure 9). However, the coupling was notably weaker in T92, which had higher stomatal conductance and A compared with other individuals. In the other trees, the coupling was tight especially at low A and g_s with an r^2 of 0.85. This tight coupling between A and g_s indicates the strong contribution that water plays in controlling assimilation rates, whereas the weaker coupling between ETR and A supports the hypothesis that alternative electron sinks decrease the coupling between electron transport and carbon assimilation. Additionally, our data support previous work showing that electron transport does not

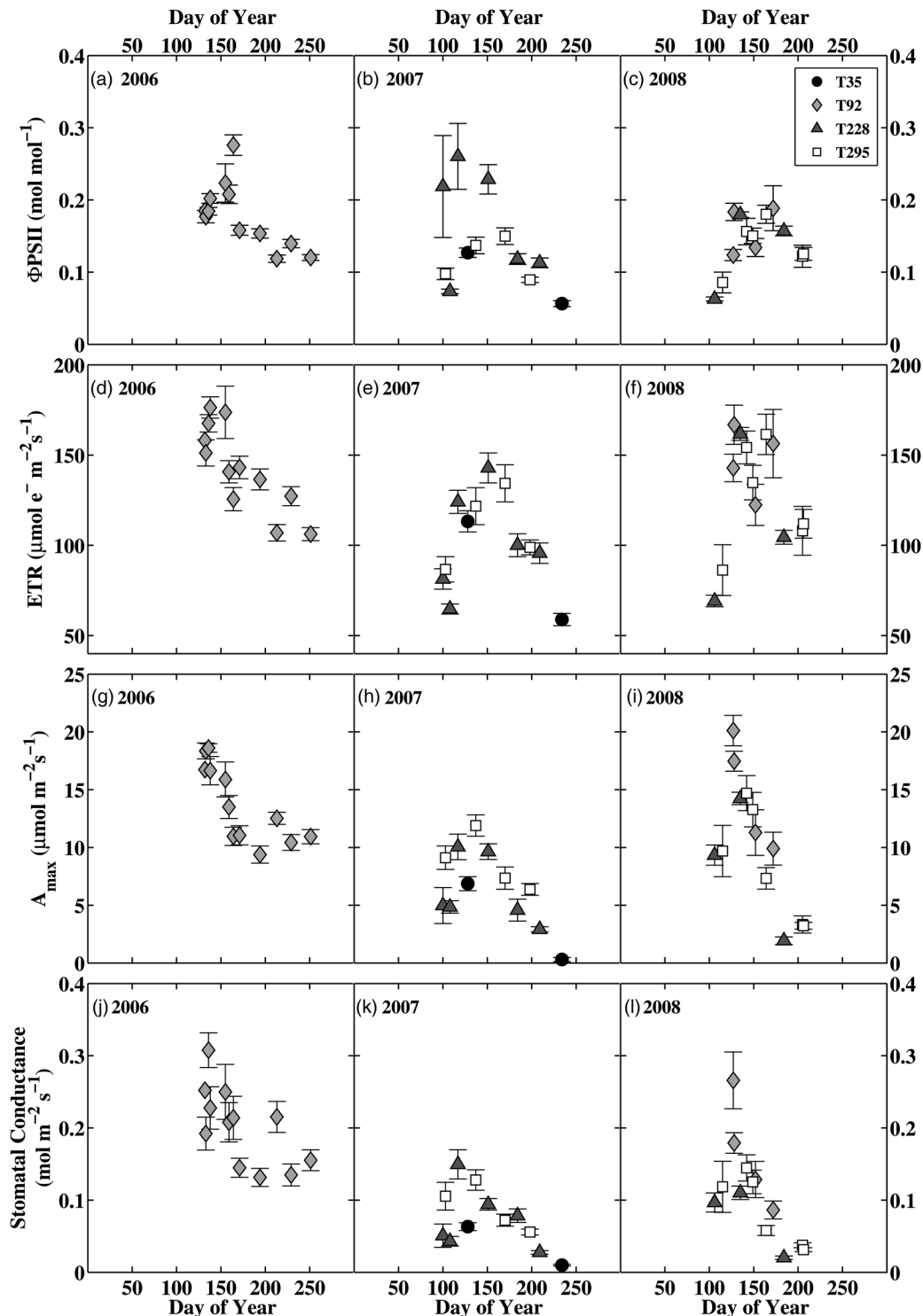


Figure 8. Data from in situ gas exchange and fluorescence measurements. Shown is the quantum yield of photosystem II (a–c), electron transport rate (d–f), instantaneous net CO₂ assimilation rate (g–i), and stomatal conductance (j–l). Data are shown from 2006 (left), 2007 (middle), and 2008 (right). Error bars indicate standard error.

necessarily decrease during drought stress when carbon assimilation decreases (Cornic 2000).

We did not observe a decrease in leaf absorbance throughout the summer drought or a significant decrease in SPAD readings. The decrease in Φ_{PSII} , however, indicates that energy

made available by chlorophyll may be directed to processes other than ATP and NADPH production in PSII. The xanthophyll cycle for non-photochemical quenching of the chlorophyll excitation may be an important process protecting blue oak leaves from over-excitation during the summer (Niyogi et al. 1998,

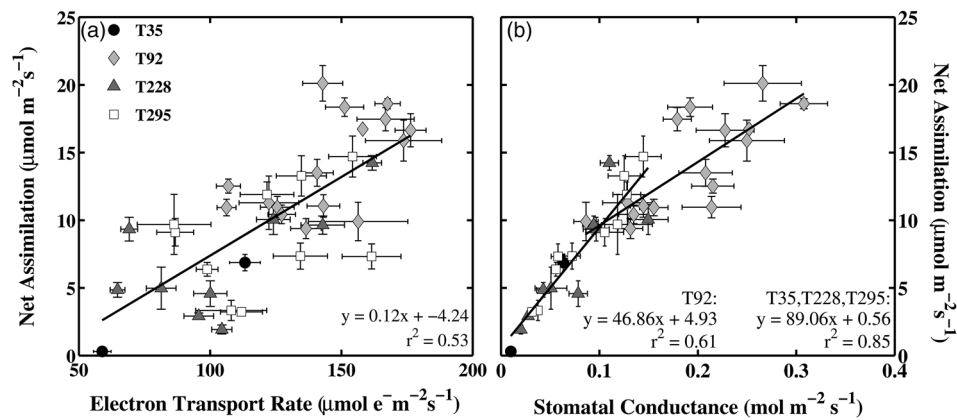


Figure 9. The correlation of net CO_2 assimilation with electron transport rate (a) and stomatal conductance (b). Data are shown for trees 35 (circles), 92 (diamonds), 228 (triangles) and 295 (squares). The regression of electron transport with net assimilation is shown for all trees and years together. The regression of stomatal conductance with net assimilation is shown separately for T92 from the remaining trees (b). Error bars indicate standard error.

Adams et al. 1999). Our work shows that the electron transport is not solely coupled to carbon assimilation.

Xu and Baldocchi (2003) concluded that a decrease in N_m and nitrogen use efficiency (NUE, mol CO_2 assimilated per gram of leaf nitrogen) resulted in the decrease in V_{cmax} . While we also observed a decrease in NUE, no summertime decrease in N_m was observed. Therefore, our data indicate that the decrease in V_{cmax} may be due to reallocation of nitrogen away from Rubisco, possibly contributing to photo-protection. More research is warranted on this topic.

Previous work reported a mean ratio of J_{max} to V_{cmax} of 1.6–1.7 across many species (Wullschlegel 1993, Medlyn et al. 2002). While T92-2006 had a fairly constant ratio ~ 2.0 in 2006, in later years the ratio decreased throughout the season (Figure 10). Because A appeared to decrease more than the ETR, the indication that J_{max} decreased more than V_{cmax} was surprising. This observation indicates that PSII may be operating with ETRs nearer to capacity than carboxylation rates—i.e., the plant maintains relatively more reserve of carboxylation capacity. Considering the increased oxygenation by Rubisco at high temperatures (Bernacchi et al. 2001), this may be part of blue oak strategy for avoiding over-excitation, but also means that if temperature decreases and/or water availability increases, leaves could capitalize on improved conditions by increasing A .

The seasonal trend of V_{cmax} observed here is consistent with the work of Xu and Baldocchi (2003); our measurements of electron transport and quantum yield of PSII also showed a peak in the spring. By normalizing A , V_{cmax} , g_s , J_{max} , ETR and ϕ_{PSII} to each's maximum value, we can compare relative down-regulation from the spring to summer. Net carbon assimilation and the measurements most closely associated— V_{cmax} and g_s —tended to decrease regularly throughout the summer, ultimately reaching $<50\%$ of peak values (Figure 11). The processes associated with converting solar radiation to energy— J_{max} , ETR

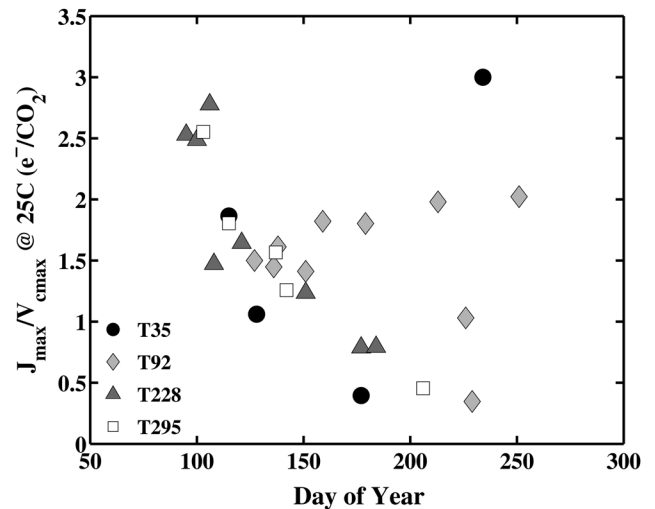


Figure 10. The ratio of maximum rate of electron transport, J_{max} , to maximum rate of carboxylation, V_{cmax} , at 25°C of trees 35 (circles), 92 (diamonds), 228 (triangles) and 295 (squares). Data shown were collected from 2006 to 2008.

and quantum yield of PSII—tended to stay $>50\%$ of the maximum throughout the summer with the exception of J_{max} , which decreased throughout the summer (as noted above). These observations reinforce the decoupling of seasonal trends of carbon assimilation with the ability to convert or dissipate solar radiation throughout. Despite reduced net CO_2 assimilation, no indication of damage to leaf pigments or photosystems that would limit A was present.

T35: the unexpected case study

As described in the Results section, we originally chose to examine T35 due to its crown's similar size and shape to T92, indicating a similar root system accessing soil moisture and ground water (Koteen et al. 2014). However, throughout 2007, the accessible leaves were decreasingly available due to early

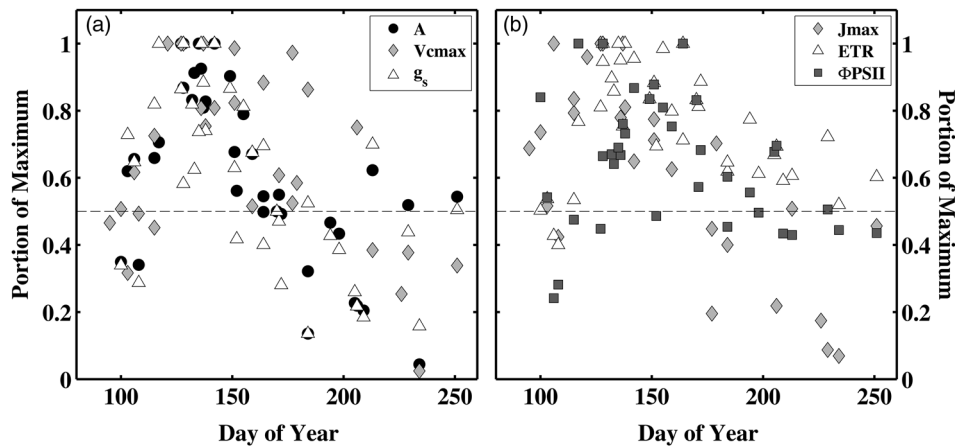


Figure 11. The seasonal trend of net CO₂ assimilation (A), maximum rate of carboxylation (V_{cmax}) and stomatal conductance (g_s) (a), and maximum and actual electron transport (J_{max} and ETR, respectively) and the quantum yield of photosystem II (ϕ_{PSII}) (b). Data are combined from four trees (T35, T92, T229, T295) and 3 years (2006–08) of measurements.

senescence soon after spring. The remaining leaves largely showed discoloration, drastically reducing the visibly healthy foliage available for sampling. This situation presented a potential bias in our measurements since the sampled leaves were the best of those remaining (in 2007) but not necessarily representative of the majority of leaves in that section of the crown. Though it was not within our original objective for this study, an additional analysis was conducted to investigate observed symptoms preceding the drastic visible changes in the crown of T35. While we cannot directly describe *why* measurements of T35 indicated damage, our results demonstrate what happens as a result.

In 2007, N_m of T35 decreased throughout the summer reaching 1.4%. N_m in T92 was significantly higher than T35 with average values of 1.99% after DOY 120–2007. This observation translated to lower SPAD readings in T35–2007. We estimated SPAD readings in 2007 from the N_m based on their linear relationship. Estimated SPAD readings of T35 in 2007 were <40 throughout nearly all of 2007, which is a distinct sign of photosynthetic impairment (Netto et al. 2005) and early senescence due to environmental stress (Buckland et al. 1991); these facts corroborate anecdotal observations during measurements. In 2008, T35 had very limited foliage accessible from the ground. The results from FLiES indicate that the sampled regions of T35 and T92 received similar amounts of incoming solar radiation, however SPAD readings from T35 were ~12 less than those of T92. Additionally, N_m of T35 was significantly less than that of T92 in 2007 and 2008 (Table 3). In 2007, N_m of T35 was significantly less than all other trees despite receiving more solar radiation than T228 throughout the period of foliation. Although we cannot distinguish the cause of low N_m in T35–2007, our observations indicate that it was associated with a breakdown in the protective mechanisms of the leaf and probably contributed to the change in foliation of the T35 crown during 2008.

In addition to T35 indicating damage in leaf structure from environmental stress, leaf function appeared affected. Peak V_{cmax} of T35 in 2007 was 82 $\mu\text{mol m}^{-2} \text{s}^{-1}$, comparable to other individuals measured the same year but lower than values previously measured in T92 (Figure 7). Most notable is that A of T35 was quite low, with a maximum of 6.9 $\mu\text{mol m}^{-2} \text{s}^{-1}$ compared with a maximum in T92 of 20.1 $\mu\text{mol m}^{-2} \text{s}^{-1}$ (Figure 8g–i). Furthermore, when V_{cmax} peaked in T35, A was <50% of the peak values of maximum A in T92. The difference between in situ rates of carbon assimilation at peak carboxylation capacity was due to the lower stomatal conductance in T35 than in T92, furthering the evidence that within-site variability in water access, most likely due to spatial heterogeneity in rock structure and soil depth, contributed to the functional differences between T35 and T92. This apparent reduction in access to water was followed by damage to leaf structures and early senescence. Early senescence has been cited previously as a method of coping with drought (Pesoli et al. 2003, Munné-Bosch and Alegre 2004).

Overall, the dynamics we observed in T35 showed that it is possible for environmental stress—most likely low water availability—to cause the breakdown in the capacity of the leaf to assimilate carbon and convert incoming solar radiation to energy. However, in the majority of trees that we measured, decreased V_{cmax} , J_{max} and g_s during the summer did not coincide with any indication of structural or biochemical damage. Electron transport rate decreased by only ~40% from the maximum, whereas V_{cmax} and J_{max} decreased by >60% each. Therefore, while blue oaks exhibit lower net carbon assimilation during the summer drought, it is not an indication of damage to the leaves.

Conclusions

Our objective in this study was to investigate the seasonal trends in carbon assimilation and the capacity to convert or dissipate PPFD in order to better understand controls over leaf

functioning throughout the annual summer drought of the California Mediterranean savanna. While one individual, T35, exhibited clear evidence of structural and biochemical damage due to stress, the remaining individuals demonstrated the maintained capacity to assimilate carbon and convert PPFD into energy, avoiding leaf damage. Thus, we determined that the reduction in net carbon assimilation during the summer drought is not a result of leaf damage but rather a result of the environmental drivers.

Other work at the site has demonstrated variability in coarse and fine root structure (Raz-Yaseef et al. 2013, Koteen et al. 2014), which would cause variable access to water. Because the blue oaks are obligate phreatophytes, transpiring mostly groundwater in the summer (Miller et al. 2010), decreased access to groundwater most likely was the primary environmental stress pushing T35 beyond the threshold to avoid leaf damage during summer drought.

The data from the remaining trees showed that electron transport and Φ_{PSII} decreased less after the spring peak period than net carbon assimilation and stomatal conductance. Thus, we conclude that environmental stress did not compromise the integrity of PSII. Further work is warranted to describe the contribution of processes such as cyclic electron transport, photorespiration, etc., that may act as alternative electron sinks and protect the blue oak leaves from damage (Ort and Baker 2002). Additionally, further work is warranted to investigate the changes in nitrogen allocation throughout the summer drought.

Because V_{cmax} is much higher than A during the summer—possibly to enable photorespiration—and because leaves are still able to convert PPFD into energy, blue oaks could be capable of increasing A if water deficits are temporarily alleviated during the summer, such as during rare precipitation pulses. This would impact the manner in which the photosynthesis precipitation pulse response is modeled in hot drought-adapted species like blue oaks. Additionally, the looser coupling between ETR and net carbon assimilation during the summer drought may impact the ability to estimate gross primary production (GPP) by remote sensing of chlorophyll fluorescence (Frankenberg et al. 2013) because it implies that in hot drought acclimated species—like those in Mediterranean climates—the fluorescence signal could become decoupled from GPP.

This work demonstrated the structural and functional effects of the large spatial heterogeneity in root structure and therefore water access at the site. Our study indicates that blue oaks are able to manage the resources and limitations during the summer drought in order to (i) achieve very high rates of net carbon assimilation when water is available, either as soil moisture or via access to groundwater, (ii) avoid structural or biochemical damage during the summer drought, (iii) avoid 'wasting' resources on unusable carboxylation or electron transport capacities and (iv) retain the ability to increase A when water stress is alleviated (i.e., during precipitation pulses).

Acknowledgments

Very sincere appreciation goes to Mr Russell Tonzi (05/04/1913–10/02/2014) for granting access to private land in support of our scientific endeavors. We thank Siyan Ma, Ted Hehn, Gretchen Miller, Xingyuan Chen, Rodrigo Vargas and Youngryel Ryu for contributions in the field. We also thank Michelle Rubin, Sonia Wharton and David Ackerly for providing helpful comments on early drafts and two anonymous reviewers for feedback that greatly improved the final manuscript. The Tonzi Ranch is a member of the AmeriFlux and Fluxnet networks.

Conflict of interest

None declared.

Funding

Funding was provided to J.L.O. through a National Science Foundation Graduate Research Fellowship and the University of California Berkeley Chancellor's Fellowship. Work was supported in part by a US Department of Energy Terrestrial Carbon Project grant DE-FG02-03ER63638 to D.D.B. Lawrence Livermore National Laboratory provided funding to J.L.O. during manuscript preparation. Lawrence Livermore National Laboratory is operated by Lawrence Livermore National Security, LLC, for the US Department of Energy, National Nuclear Security Administration under Contract DE-AC52-07NA27344 and LLNL-JRNL-664018.

References

- Adams WW III, Demmig-Adams B, Logan BA, Barker DH, Osmond CB (1999) Rapid changes in xanthophyll cycle-dependent energy dissipation and photosystem II efficiency in two vines, *Stephania japonica* and *Smilax australis*, growing in the understory of an open *Eucalyptus* forest. *Plant Cell Environ* 22:125–136.
- Baldocchi DD, Xu L, Kiang N (2004) How plant functional-type, weather, seasonal drought, and soil physical properties alter water and energy fluxes of an oak–grass savanna and an annual grassland. *Agric For Meteorol* 123:13–39.
- Baldocchi D, Tang J, Xu L (2006) How switches and lags in biophysical regulators affect spatial-temporal variation of soil respiration in an oak-grass savanna. *J Geophys Res* 111:G02008. doi:10.1029/2005JG000063.
- Bernacchi CJ, Singaas EL, Pimentel C, Portis AR Jr, Long SP (2001) Improved temperature response functions for models of Rubisco-limited photosynthesis. *Plant Cell Environ* 24:253–259.
- Buckland SM, Price AH, Hendry GAF (1991) The role of ascorbate in drought-treated *Cochlearia atlantica* Poved. and *Armeria maritima* (Mill.) Willd. *New Phytol* 119:155–160.
- Cayan DR, Maurer EP, Dettinger MD, Tyree M, Hayhoe K (2008) Climate change scenarios for the California region. *Clim Change* 87:21–42.
- Chen Q, Baldocchi D, Gong P, Dawson T (2008a) Modeling radiation and photosynthesis of a heterogeneous savanna woodland landscape with a hierarchy of model complexities. *Agric For Meteorol* 148:1005–1020.

- Chen X, Rubin Y, Ma S, Baldocchi D (2008b) Observations and stochastic modeling of soil moisture control on evapotranspiration in a Californian oak savanna. *Water Resour Res* 44:W08409.
- Cornic G (2000) Drought stress inhibits photosynthesis by decreasing stomatal aperture—not by affecting ATP synthesis. *Trends Plant Sci* 5:187–188.
- Dai A, Meehl GA, Washington WM, Wigley TML, Arblaster JM (2001) Ensemble simulation of twenty-first century climate changes: business-as-usual versus CO₂ stabilization. *Bull Am Meteorol Soc* 82:2377–2388.
- Damesin C, Rambal S (1995) Field study of leaf photosynthetic performance by a Mediterranean deciduous oak tree (*Quercus pubescens*) during a severe summer drought. *New Phytol* 131:159–167.
- Damesin C, Rambal S, Joffre R (1998) Co-occurrence of trees with different leaf habit: a functional approach on Mediterranean oaks. 19:195–204.
- Damour G, Vandame M, Urban L (2009) Long-term drought results in a reversible decline in photosynthetic capacity in mango leaves, not just a decrease in stomatal conductance. *Tree Physiol* 29:675–684.
- Farquhar GD, von Caemmerer S, Berry JA (1980) A biochemical model of photosynthetic CO₂ assimilation in leaves of C₃ species. *Planta* 149:78–90.
- Frankenberg C, Berry J, Guanter L, Joiner J (2013) Remote sensing of terrestrial chlorophyll fluorescence from space. *SPIE Newsroom* 2–5. doi:10.1117/2.1201302.004725.
- Genty B, Briantais J-M, Baker NR (1989) The relationship between the quantum yield of photosynthetic electron transport and quenching of chlorophyll fluorescence. *Biochim Biophys Acta* 990:87–92.
- Hamerlynck EP, Huxman TE, Loik ME, Smith SD (2000) Effects of extreme high temperature, drought and elevated CO₂ on photosynthesis of the Mojave Desert evergreen shrub, *Larrea tridentata*. *Plant Ecol* 148:183–193.
- Harley PC, Thomas RB, Reynolds JF, Strain BR (1992) Modelling photosynthesis of cotton grown in elevated CO₂. *Plant Cell Environ* 15:271–282.
- Kobayashi H, Iwabuchi H (2008) A coupled 1-D atmosphere and 3-D canopy radiative transfer model for canopy reflectance, light environment, and photosynthesis simulation in a heterogeneous landscape. *Remote Sens Environ* 112:173–185.
- Kobayashi H, Baldocchi DD, Ryu Y, Chen Q, Ma S, Osuna JL, Ustin SL (2012) Modeling energy and carbon fluxes in a heterogeneous oak woodland: a three-dimensional approach. *Agric For Meteorol* 152:83–100.
- Koteen LE, Raz-Yaseef N, Baldocchi DD (2014) Spatial heterogeneity of fine root biomass and soil carbon in a California oak savanna illuminates plant functional strategy across periods of high and low resource supply. *Ecology* 8:294–308.
- Kueppers LM, Snyder MA, Sloan LC, Zavaleta ES, Fulfrost B (2005) Modeled regional climate change and California endemic oak ranges. *Proc Natl Acad Sci USA* 102:16281–16286.
- Lawlor DW, Tezara W (2009) Causes of decreased photosynthetic rate and metabolic capacity in water-deficient leaf cells: a critical evaluation of mechanisms and integration of processes. *Ann Bot* 103:561–579.
- Limousin J-M, Misson L, Lavoie A-V, Martin NK, Rambal S (2010) Do photosynthetic limitations of evergreen *Quercus ilex* leaves change with long-term increased drought severity? *Plant Cell Environ* 33:863–875.
- Ma S, Baldocchi DD, Xu L, Hehn T (2007) Inter-annual variability in carbon dioxide exchange of an oak/grass savanna and open grassland in California. *Agric For Meteorol* 147:157–171.
- Ma S, Baldocchi DD, Mambelli S, Dawson TE (2011) Are temporal variations of leaf traits responsible for seasonal and inter-annual variability in ecosystem CO₂ exchange? *Funct Ecol* 25:258–270.
- Marshall B, Biscoe PV (1980) A model for C₃ leaves describing the dependence of net photosynthesis on irradiance. *J Exp Bot* 31:29–39.
- Martínez-Ferri E, Balaguer L, Valladares F, Chico JM, Manrique E (2000) Energy dissipation in drought-avoiding and drought-tolerant tree species at midday during the Mediterranean summer. *Tree Physiol* 20:131–138.
- Medlyn BE, Dreyer E, Ellsworth D et al. (2002) Temperature response of parameters of a biochemically based model of photosynthesis. II. A review of experimental data. *Plant Cell Environ* 25:1167–1179.
- Miao Z, Xu M, Lathrop RG Jr, Wang Y (2009) Comparison of the A-Cc curve fitting methods in determining maximum ribulose 1.5-bisphosphate carboxylase/oxygenase carboxylation rate, potential light saturated electron transport rate and leaf dark respiration. *Plant Cell Environ* 32:109–122.
- Miller GR, Chen X, Rubin Y, Ma S, Baldocchi DD (2010) Groundwater uptake by woody vegetation in a semiarid oak savanna. *Water Resour Res* 46:W10503.
- Misson L, Limousin J-M, Rodriguez R, Letts MG (2010) Leaf physiological responses to extreme droughts in Mediterranean *Quercus ilex* forest. *Plant Cell Environ* 33:1898–1910.
- Munné-Bosch S, Alegre L (2004) Die and let live: leaf senescence contributes to plant survival under drought stress. *Funct Plant Biol* 31:203–216.
- Netto AT, Campostrini E, de Oliveira JG, Bressan-Smith RE (2005) Photosynthetic pigments, nitrogen, chlorophyll a fluorescence and SPAD-502 readings in coffee leaves. *Sci Hortic (Amsterdam)* 104:199–209.
- Niyogi KK, Grossman AR, Björkman O (1998) *Arabidopsis* mutants define a central role for the xanthophyll cycle in the regulation of photosynthetic energy conversion. *Plant Cell* 10:1121–1134.
- Ort DR, Baker NR (2002) A photoprotective role for O₂ as an alternative electron sink in photosynthesis? *Curr Opin Plant Biol* 5:193–198.
- Pesoli P, Gratani L, Larcher W (2003) Responses of *Quercus ilex* from different provenances to experimentally imposed water stress. *Biol Plant* 46:577–581.
- Raz-Yaseef N, Koteen L, Baldocchi DD (2013) Coarse root distribution of a semi-arid oak savanna estimated with ground penetrating radar. *J Geophys Res Biogeosci* 118:135–147.
- Ryu Y, Sonnentag O, Nilson T, Vargas R, Kobayashi H, Wenk R, Baldocchi DD (2010) How to quantify tree leaf area index in an open savanna ecosystem: a multi-instrument and multi-model approach. *Agric For Meteorol* 150:63–76.
- Ryu Y, Verfaillie J, Macfarlane C, Kobayashi H, Sonnentag O, Vargas R, Ma S, Baldocchi DD (2012) Continuous observation of tree leaf area index at ecosystem scale using upward-pointing digital cameras. *Remote Sens Environ* 126:116–125.
- Sharkey TD, Bernacchi CJ, Farquhar GD, Singaas EL (2007) Fitting photosynthetic carbon dioxide response curves for C₃ leaves. *Plant Cell Environ* 30:1035–1040.
- Tenhunen JD, Lange OL, Harley PC, Beyschlag W, Meyer A (1985) Limitations due to water stress on leaf net photosynthesis of *Quercus coccifera* in the Portuguese evergreen scrub. *Oecologia* 67:23–30.
- Tenhunen JD, Serra AS, Harley PC, Dougherty RL, Reynolds JF (1990) Factors influencing carbon fixation and water use by mediterranean sclerophyll shrubs during summer drought. *Oecologia* 82:381–393.
- Thornley JHM, Johnson IR (1990) Plant and crop modelling: a mathematical approach to plant and crop physiology. Oxford University Press, New York, NY.
- Vargas R, Sonnentag O, Abramowitz G et al. (2013) Drought influences the accuracy of simulated ecosystem fluxes: a model-data meta-analysis for Mediterranean oak woodlands. *Ecosystems* 16:749–764.
- Von Caemmerer S (2000) Biochemical models of leaf photosynthesis. Techniques in plant sciences. CSIRO Publishing, Collingwood, VIC, Australia.
- Werner C, Ryel RJ, Correia O, Beyschlag W (2001) Effects of photoinhibition on whole-plant carbon gain assessed with a photosynthesis model. *Plant Cell Environ* 24:27–40.
- Wright IJ, Reich PB, Westoby M et al. (2004) The worldwide leaf economics spectrum. *Nature* 428:821–827.

- Wullschlegel SD (1993) Biochemical limitations to carbon assimilation in C_3 plants—a retrospective analysis of the A/C_i curves from 109 species. *J Exp Bot* 44:907–920.
- Xu L, Baldocchi DD (2003) Seasonal trends in photosynthetic parameters and stomatal conductance of blue oak (*Quercus douglasii*) under prolonged summer drought and high temperature. *Tree Physiol* 23:865–877.
- Xu L, Baldocchi DD (2004) Seasonal variation in carbon dioxide exchange over a Mediterranean annual grassland in California. *Agric For Meteorol* 123:79–96.
- Zeiger E, Iino M, Ogawa T (1985) The blue light response of stomata: pulse kinetics and some mechanistic implications. *Photochem Photobiol* 42:759–763.